

Deposition and characterization of TiZrV-Pd thin films by dc magnetron sputtering^{*}

WANG Jie(王洁) ZHANG Bo(张波)¹⁾ XU Yan-Hui(徐延辉) WEI Wei(尉伟)
FAN Le(范乐) PEI Xiang-Tao(裴香涛) HONG Yuan-Zhi(洪远志) WANG Yong(王勇)

National Synchrotron Radiation Laboratory, University of Science and Technology of China, Hefei 230029, China

Abstract: TiZrV film is mainly applied in the ultra-high vacuum pipes of storage rings. Thin film coatings of palladium, which are added onto the TiZrV film to increase the service life of nonevaporable getters and enhance H₂ pumping speed, were deposited on the inner face of stainless steel pipes by dc magnetron sputtering using argon gas as the sputtering gas. The TiZrV-Pd film properties were investigated by atomic force microscope (AFM), scanning electron microscope (SEM), X-ray photoelectron spectroscopy (XPS) and X-Ray Diffraction (XRD). The grain size of TiZrV and Pd films were about 0.42–1.3 nm and 8.5–18.25 nm respectively. It was found that the roughness of TiZrV films is small, about 2–4 nm, but for Pd film it is large, about 17–19 nm. The PP At. % of Pd in TiZrV/Pd films varied from 86.84 to 87.56 according to the XPS test results.

Key words: TiZrV-Pd, nonevaporable getters, film coating, dc magnetron sputtering

PACS: 29.20.-c **DOI:** 10.1088/1674-1137/39/12/127007

1 Introduction

Titanium-Zirconium-Vanadium (TiZrV) is a nonevaporable getter (NEG) [1–4] which has been extensively studied during the past two decades for low secondary electron yield [5–7] and for its sorption properties with many gases such as hydrogen, oxygen, nitrogen, carbon monoxide and dioxide. The sorption of these gases, except for H₂, is not reversible and causes a progressive contamination of the TiZrV film [1, 8, 9]. Moreover, repeated air exposure–activation cycles progressively enrich the film with reactive gases, reducing its performance and shortening its operating life [10]. In order to enhance the lifetime of TiZrV film, a palladium overlayer is added to it. The contribution of the thin palladium film is particularly relevant to the pumping of hydrogen gas, due to its high sticking factor on palladium and the great sorption capacity of the underlying TiZrV getter.

Several researchers have studied the absorbing behavior of TiZrV-Pd. Mura et al. [11, 12] designed an ion pump internally coated by TiZrV-Pd film, based on technology licensed to them by CERN (European Center for Nuclear Research). The results showed that the pumping speed for H₂ was an order of magnitude higher, owing to the contribution of the getter. In addition, Ben-

venuti et al. [13] studied the electron stimulated desorption and pumping speed measurements of TiZrV-Pd at CERN for particle accelerator applications. Nonetheless, it is necessary to have further study into the effect of the coating process and parameters such as discharge current, discharge voltage, working pressure etc. on the film structure, surface topography and grain size in the dc magnetron sputtering process. Therefore, the aim of this paper is to study these problems.

Several years ago, the composition, structure and second electron yields (SEY) of TiZrV film were studied in our group [14]. However, the effect of the coating process and parameters such as gas flow and working pressure on the TiZrV film structure, surface topography and grain size in the dc magnetron sputtering process were not studied. Moreover, in order to enhance the lifetime of TiZrV film and increase the pumping capacity of hydrogen gas, the deposition and characterization of Pd film are illustrated in this article.

2 Experiment

2.1 Coating equipment

A magnetron sputtering system was designed to coat TiZrV-Pd film onto the inner surface of a stainless steel

Received 2 April 2015

^{*} Supported by National Natural Science Funds of China (11205155) and Fundamental Research Funds for the Central Universities (WK2310000041)

1) E-mail: zhbo@ustc.edu.cn

©2015 Chinese Physical Society and the Institute of High Energy Physics of the Chinese Academy of Sciences and the Institute of Modern Physics of the Chinese Academy of Sciences and IOP Publishing Ltd

pipe using argon as the sputtering gas, as shown in Fig. 1. This deposition system is similar to the one introduced in Ref. [14]. However, the difference here is that there are two cathodes which are used one-by-one. One cathode is made from twisting together Ti, Zr and V wires (2 mm in diameter) and the other is Pd wire (1 mm in diameter). Ten minutes was needed for the exchange of cathode wires. There is a ceramic insulation on top of the feedthrough. A ceramic cylinder is fixed at the end of the cathode to keep it insulated from the interior wall. In order to ensure the uniformity of film thickness, the cathode filament was fixed in the center of the stainless steel pipe using a bellows transmission mechanism (Fig. 1). Before deposition, Si substrates were cleaned by the same method presented in Ref. [14].

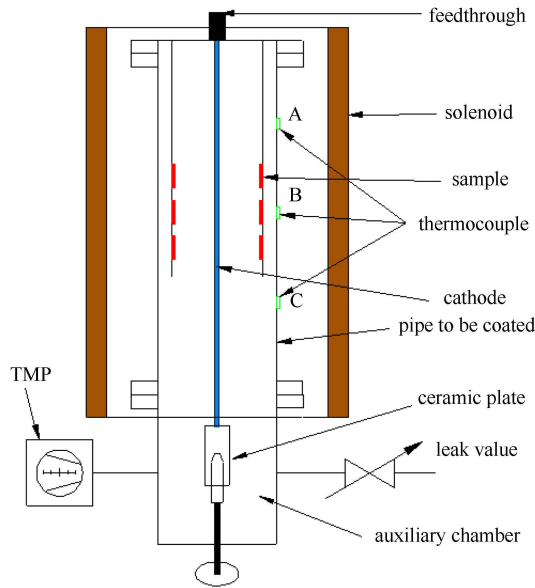


Fig. 1. (color online) Schematic diagram of TiZrV-Pd deposition system.

2.2 Magnetron sputtering process

Generally speaking, the NEG-Pd film coating process was divided into three steps. Firstly, the TiZrV wires cathode was powered on with the selected film coating parameters. Secondly, after TiZrV film coating, nitrogen was passed into the pipeline before opening the flange. Thirdly, the Pd wire cathode was installed as quickly as possible, then film coating was started.

The roughness and porosity of TiZrV-Pd coatings increased with substrate temperature during deposition. Moreover, a rougher film surface can absorb more pollution gases such as carbon dioxide and oxygen. Consequently, the substrates were not intentionally heated during deposition. Three thermocouples were used to measure the temperature of the pipe wall, as shown in Fig. 1. The temperature varied from 60 °C to 120 °C

for TiZrV film coating with different sputtering current, while the temperature varied from 30 °C to 100 °C for Pd film coating. In Fig. 1, the temperature at point B was the highest, owing to the worst heat dissipation being in the center of the solenoid, which has no cooling system. The temperature at point A was higher than point C on account of the hot feedthrough during the film coating process.

2.3 Characterization method

Film morphology was measured by use of a Sirion 200 Schottky field scanning electron microscope (SEM). The composition was obtained with a Thermo ESCALAB 250 X-ray photoelectron spectrometer (XPS). The spectrometer was equipped with a hemispherical analyzer and a monochromator, with a beam spot size of 500 μm. All XPS data was measured with Al Kα X-rays with ($h\nu=1486.6$ eV) operated at 150 W and an analyzer at 45 degrees. Surface morphology was observed through an Innova atomic force microscope (AFM) at room temperature. The crystal structure and the size of the crystallites was obtained by Rigaku TTR-III X-Ray Powder Diffraction (XRD). All XRD data was tested with Cu Kα X-rays which were used at 40 kV/200 mA. In addition, a diffractometer was used in a $2\theta/\theta$ mode, 2θ varying from 30 to 90 with a 0.02 step.

3 Results and discussion

3.1 Structural characterization

Peak width is mainly affected by the following four factors: uncertainty of wavelength, grain size, the position of instruments and samples, and micro stress that exists within the scope of one or a few grains and keeps the balance of internal stress. Of the four factors, only the grain size was considered as the reason for peak widening and the other factors were ignored. Under the assumption of a homogeneous single phase and roughly equiaxial crystal grains, the Scherrer formula was applied to determine the average dimension of the crystallites:

$$D = \frac{k\lambda}{W_{1/2} \cos\theta_B},$$

where k is Scherrer's constant, which depends on the crystal shape and is related to grain size and distribution, often having a value of 0.89; λ is the wavelength of the source, i.e. 0.154 nm for copper Kα; $W_{1/2}$ is the angle in radians of the full width at half maximum (FWHM); θ_B is the diffraction angle in degrees; and D is the grain size.

According to the XRD test results, the grain size of TiZrV films was about 0.42 nm (Sample #9-TiZrV) to 1.3 nm (Sample #2-TiZrV), as shown in Fig. 2. The grain size of Pd films was 8.5 nm (Sample #6-Pd) to

Table 1. Film coating parameters.

| sample | discharge voltage/V | discharge current/A | working pressure/Pa | magnetic field/ $\times 10^4$ T | gas flow/Scm |
|----------|---------------------|---------------------|---------------------|---------------------------------|--------------|
| #1-TiZrV | 492-343 | 0.5 | 2.0 | 175 | 2.0 |
| #1-Pd | 530-523 | 0.04 | 2.0 | 175 | 2.0 |
| #2-TiZrV | 508-561 | 0.2 | 2.0 | 93 | 2.0 |
| #2-Pd | 444-453 | 0.02 | 2.0 | 235 | 2.0 |
| #3-TiZrV | 511-524 | 0.2 | 0.8 | 230 | 1.2 |
| #3-Pd | 430-440 | 0.02 | 2.0 | 206 | 2.0 |
| #4-TiZrV | 544-552 | 0.2 | 7.0 | 70 | 2.0 |
| #4-Pd | 443-440 | 0.02 | 2.0 | 64 | 2.0 |
| #5-Pd | 424-458 | 0.02 | 2.0 | 175 | 1.0 |
| #6-Pd | 329-354 | 0.2 | 20.0 | 123 | 2.0 |
| #7-TiZrV | 327-378 | 0.25 | 2.0 | 123 | 1.0 |
| #7-Pd | 437-548 | 0.04 | 5.0 | 175 | 2.0 |
| #8-Pd | 464-573 | 0.04 | 20.0 | 175 | 2.0 |
| #9-TiZrV | 400-347 | 0.25 | 2.0 | 123 | 4.0 |
| #10-Pd | 413-428 | 0.02 | 2.0 | 175 | 2.0 |
| #11-Pd | 432-440 | 0.02 | 2.0 | 232 | 2.0 |
| #12-Pd | 456-527 | 0.04 | 10.0 | 175 | 2.0 |

18.25 nm (Sample #2- Pd), as shown in Fig. 3. Under the same coating conditions, the type of substrate has little effect on the grain size of Pd film. For instance, the grain size of Pd film deposited on TiZrV film was 14.9 nm, and the one on silicon (Si<111>) was 12.7 nm for sample #10-Pd. Furthermore, the film coating parameters of the samples are listed in Table 1. Possible causes are as follows. For the first Pd layer, different substrates will have an obvious impact on their arrangement. When the number of Pd atomic layers increases, this effect of substrate on Pd layers is weakened little by little. On average, the effect of substrates on the grain size of Pd film is small, according to the test results which are shown in Table 2.

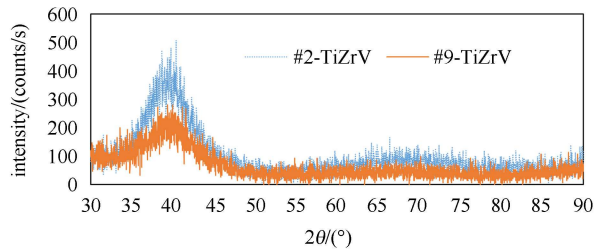


Fig. 2. (color online) X-ray diffraction of TiZrV films deposited under different film coating conditions.

3.2 Surface morphology and section morphology

The section morphology of samples #1-TiZrV and #1-Pd are shown in Fig. 4. It is clear that the roughness of the TiZrV films is small, mainly about 2–4 nm, and that of Pd film is large, about 17–19 nm. The deposition rates of samples #1-TiZrV and #1-Pd were 326 nm/h and 185 nm/h, respectively. It can be inferred from the

SEM measurement that the grain size of the TiZrV film is lower than that of the Pd film.

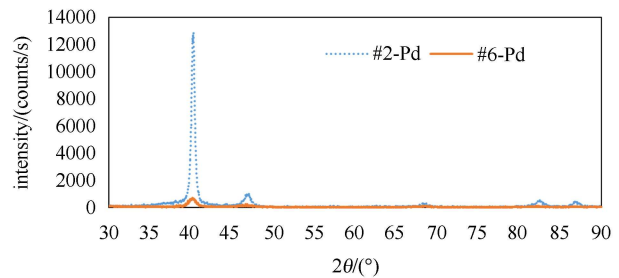


Fig. 3. (color online) X-ray diffraction of films comparing TiZrV/Pd films deposited under different film coating conditions.

Table 2. The grain size of Pd film on different substrates according to XRD test results.

| sample | grain size/nm (silicon-substrate) | grain size/nm (TiZrV-substrate) | the thickness of Pd film/nm |
|--------|--------------------------------------|------------------------------------|-----------------------------------|
| #10-Pd | 14.9 | 12.7 | 160 |
| #11-Pd | 17.4 | 17.3 | 220 |
| #8-Pd | 16.1 | 14.5 | 230 |
| #12-Pd | 12.3 | 13.1 | 270 |
| #7-Pd | 12.3 | 13.7 | 400 |

The surface of the TiZrV film deposited on silicon was smooth and the largest degree of roughness was 3.6 nm with a scanning range of 5 μm , as shown in Fig. 5(a). The surface of Pd film deposited on silicon was rough compared with the one on TiZrV film, and the degree of roughness was roughly 15.9 nm as shown in Fig. 5(b). Furthermore, the roughness of Pd film deposited on TiZrV film was slightly larger than on silicon

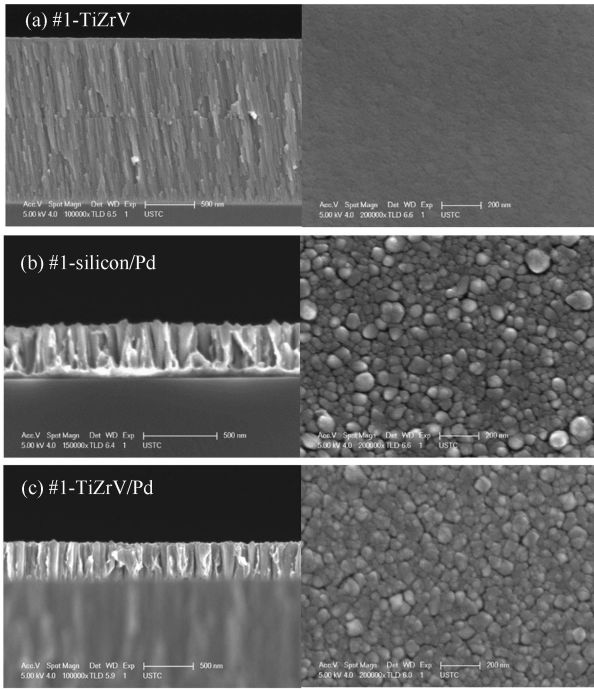


Fig. 4. (color online) Cross section morphology (left) and surface topography (right) of TiZrV film deposited on silicon by SEM for (a), Pd film deposited on silicon and (b), Pd film deposited on TiZrV film. The film coating parameters were the same for Pd film in (b) and (c).

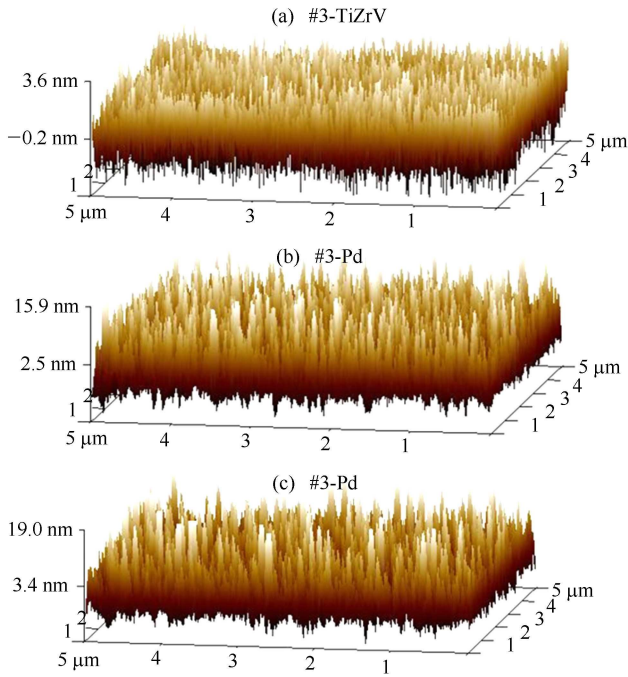


Fig. 5. (color online) AFM images of (a) TiZrV film deposited on silicon, (b) Pd film deposited on silicon, and (c) Pd film deposited on TiZrV film. The film coating parameters were the same for Pd film in (b) and (c).

wafer, roughly 19.0 nm, as shown in Fig. 5(c). Therefore, for the same silicon substrate, the roughness of TiZrV films was higher than Pd film under different film coating processes. It is likely that the main factor influencing the film surface roughness was the nature of the film rather than the substrates, based on the AFM test results.

Under the conditions of discharge current 0.25 A, operating pressure 2.0 Pa, magnetic field strength 1.23×10^{-2} T, and gas flow changing between 1.0 and 4.0 Sccm, AFM images of TiZrV film are shown in Fig. 6. It is obvious that the influence of gas flow on TiZrV film roughness is negligible.

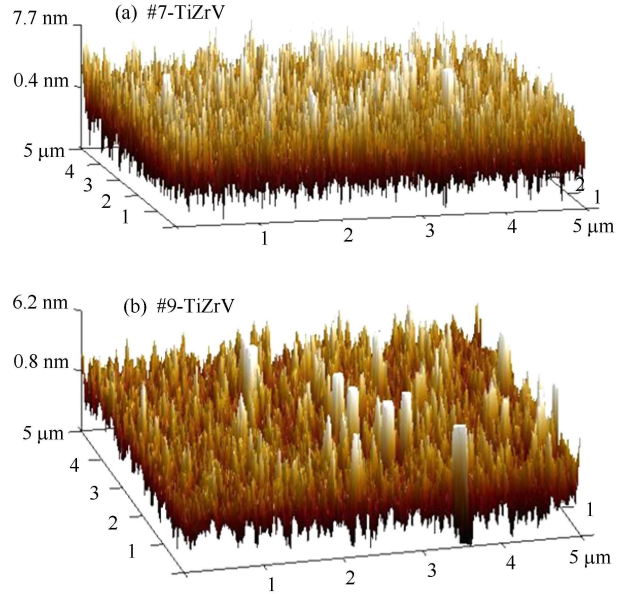


Fig. 6. (color online) AFM images of TiZrV film deposited on silicon at (a) 1.0 Sccm, and (b) 4.0 Sccm gas flow, under the condition of discharge current 0.25 A, operating pressure 2.0 Pa, and magnetic field strength 1.23×10^{-2} T.

Table 3. Ratios of elements in TiZrV films based on XPS.

| sample (TiZrV film) | Ti:Zr:V |
|---------------------|-------------|
| #4-TiZrV | 2.4:2.8:4.8 |
| #7-TiZrV | 1.6:1.1:7.3 |
| #9-TiZrV | 1.4:1.1:7.5 |

3.3 Film composition analysis

After exposure to the atmosphere, a few nanometers of passivation layer, which is mainly composed of oxide, carbide and nitride, will form on the surface of the getter film. Figure 7 illustrates that O had the highest atomic number percentage, C the second, and N the lowest in the TiZrV film samples. Furthermore, V was mainly in the form of V_2O_3 because the binding energy of V is

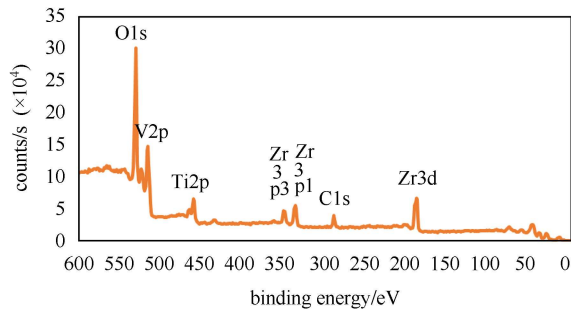


Fig. 7. (color online) XPS spectrogram of sample #4-TiZrV.

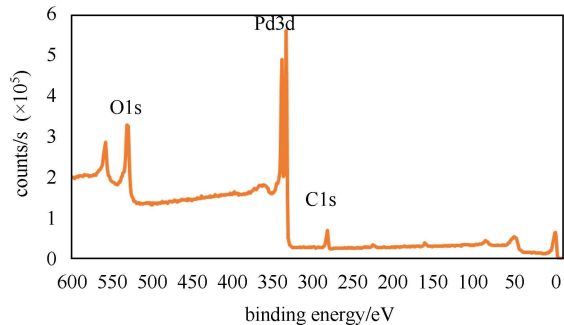


Fig. 8. (color online) XPS spectrogram of sample #4-Pd.

516 eV. The peaks at around 459 eV, produced by TiO_2 , show that air-exposed TiZrV film was partially oxidized. Table 3 shows the ratios of elements in the TiZrV films based on the XPS results.

The XPS of the air-exposed Pd film is shown in Fig. 8. The oxygen peaks at around 531 eV show that the air-

exposed Pd film was contaminated in the process of sample transfer. The carbon peaks at 284 eV show traces of organic carbon pollution, very similar to that usually noticed for metal surfaces of a different nature. In addition, the PP At. % of Pd in the Pd films varied from 86.84 to 87.56 based on the XPS.

4 Conclusions

Various surface-sensitive analysis techniques were used to study the deposition and characterization of TiZrV-Pd film prepared by dc magnetron sputtering.

SEM and AFM test results consistently show that the TiZrV films had a highly consistent thickness, while there were obvious fluctuations in the thickness of Pd film. Moreover, the roughness of TiZrV films deposited on silicon were 3.6–5.0 nm with a scanning range of 5 μm , while that of Pd films was rougher, those deposited on TiZrV film and silicon being almost the same at about 15.0–26.0 nm. Generally, the greater the working pressure, the greater the roughness of the film surface was, under the same gas flow, magnetic field strength and discharge current condition. In order to obtain high quality films, it is necessary to improve the vacuum purity of the system, since residual gases were adsorbed by the surface of the films in the vacuum chamber during the process of film coating. The ratio of Ti, Zr and V varied between 2.4:2.8:4.8 and 1.1:1.6:7.3 in TiZrV films. In addition, the PP At. % of Pd in TiZrV/Pd films varied from 86.84 to 87.56.

References

- Benvenuti C, Chiggiato P, Mongelluzzo A, Prodromides A, Ruzinov V, Scheuerlein C, Taborelli M, Levy F. *Journal of Vacuum Science & Technology A: Vacuum, Surfaces, and Films*, 2001, **19**(6): 2925
- Drbohlav J, Matolin V. *Vacuum*, 2003, **71**(1–2): 323
- Ferreira M J, Seraphim R M, Ramirez A J, Tabacniks M H, Nascente P A P. *Physcs Proc.*, 2012, **32**: 840
- Sutara F, Skala T, Masek K, Matolin V. *Vacuum*, 2009, **83**(5): 824
- Pimpec F Le, Kirby R E, King F K, Pivi M. *Nuclear Instruments and Methods in Physics Research Section A: Accelerators, Spectrometers, Detectors and Associated Equipment*, 2006, **564**(1): 44
- Suetsugu Y, Kanazawa K, Shibata K, Hisamatsu H, Oide K, Takasaki F, Dostovalov R V, Krasnov A A, Zolotarev K V, Konstantinov E S, Chernov V A, Bondar A E, Shmakov A N. *Accelerators, Spectrometers, Detectors and Associated Equipment*, 2005, **554**(1–3): 92
- Pimpec F Le, Kirby R E, King F, Pivi M. *Nuclear Instruments and Methods in Physics Research Section A: Accelerators, Spectrometers, Detectors and Associated Equipment*, 2005, **551**(2–3): 187
- Anashin V V, Collins I R, Dostovalov R V, Fedorov N V, Krasnov A A, Malyshev O B, Ruzinov V L. *Vacuum*, 2004, **75**(2): 155
- Mahner E, Hansen J, Kühler D, Malabaila M, Taborelli M. *Physical Review Special Topics-Accelerators and Beams*, 2005, **8**(5):
- Drbohlav J, Matolinova I, Masek K, Matolin V. *Vacuum*, 2005, **80**(1–3): 47
- Mura M, Paolini C. *Vakuum in Forschung und Praxis*, 2007, **19**(4): 13
- Paolini C, Mura M, Ravelli F. *Journal of Vacuum Science & Technology A: Vacuum, Surfaces, and Films*, 2008, **26**(4): 1037
- Benvenuti C, Chiggiato P, Cicoira F, Aminot Y L, Ruzinov V. *Vacuum*, 2004, **73**(2): 139
- WANG Yong et al. *Proceedings of PAC09*. Vancouver, BC, Canada. <http://epaper.kek.jp/PAC2009/papers/mo6rfp024.pdf>